

CHEMISTRY

A European Journal



Accepted Article

Title: On the Metal Cooperativity in a Dinuclear Copper-Guanidine Complex for aliphatic C–H Bond Cleavage by Dioxygen

Authors: Florian Schön, Florian Biebl, Lutz Greb, Simone Leingang, Benjamin Grimm-Lebsanft, Melissa Teubner, Soeren Buchenau, Elisabeth Kaifer, Michael Alexander Rübhausen, and Hans-Jörg Himmel

This manuscript has been accepted after peer review and appears as an Accepted Article online prior to editing, proofing, and formal publication of the final Version of Record (VoR). This work is currently citable by using the Digital Object Identifier (DOI) given below. The VoR will be published online in Early View as soon as possible and may be different to this Accepted Article as a result of editing. Readers should obtain the VoR from the journal website shown below when it is published to ensure accuracy of information. The authors are responsible for the content of this Accepted Article.

To be cited as: *Chem. Eur. J.* 10.1002/chem.201901906

Link to VoR: <http://dx.doi.org/10.1002/chem.201901906>

Supported by
ACES

WILEY-VCH

On the Metal Cooperativity in a Dinuclear Copper-Guanidine Complex for aliphatic C–H Bond Cleavage by Dioxygen

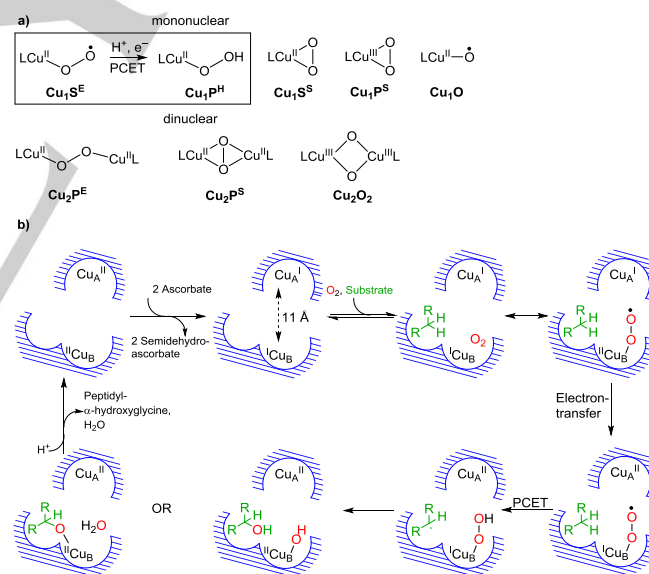
F. Schön,^[a] F. Biebl,^[b] L. Greb,^[a] S. Leingang,^[a] B. Grimm-Lebsanft,^[b] M. Teubner,^[b] Sören Buchenau,^[b] E. Kaifer,^[a] M. A. Rübhausen,^[b] H.-J. Himmel^{*[a]}

Abstract: Selective oxidation reactions of organic compounds with dioxygen using molecular copper complexes are of relevance for synthetic chemistry as well as enzymatic reactivity. In the enzyme peptidylglycine α -hydroxylating monooxygenase (PHM), the aliphatic substrate hydroxylating activity arises from the cooperative effect between two copper atoms, but the detailed mechanism is still not completely clarified. Herein we report on a model complex, for which an aliphatic ligand hydroxylation initiated by dioxygen is observed. According to DFT calculations, the proton-coupled electron transfer (PCET) process leading to ligand hydroxylation benefits from cooperative effects between the two copper atoms in this complex. While one copper atom is responsible for dioxygen binding and activation, the other stabilizes the product of intramolecular PCET by copper-ligand charge-transfer. The results of this work might pave the way for the directed utilization of cooperative effects in oxidation reactions.

Introduction

The distinguished ability of copper complexes to activate dioxygen has long been recognized.^[1–8] Nature has developed a number of copper-containing oxidase enzymes with hugely varying binding modes of dioxygen to the copper in their active centers,^[9–17] the most common ones being sketched in Scheme 1a. There are examples of well characterized, mononuclear copper(II) *end-on* superoxo^[18–23] ($\text{Cu}_1\text{S}^{\text{E}}$) or *side-on* (μ^2) superoxo^[24–27] ($\text{Cu}_1\text{S}^{\text{S}}$) complexes, and also copper(III) side-on (μ^2) peroxy^[28] ($\text{Cu}_1\text{P}^{\text{S}}$) complexes. However, in the literature there is still a lack of copper complexes that mimic the structure or the reactivity of enzymes such as tyramine β -monooxygenase (T β M), dopamine β -monooxygenase (D β M) or peptidylglycine α -hydroxylating monooxygenase (PHM). Several studies^[29, 30] suggested a $\text{Cu}_1\text{S}^{\text{E}}$ species as the key reactive intermediate in aliphatic substrate hydroxylating activity of these enzymes, in which the active sites consist of two differently bound copper

atoms (denoted as Cu_A and Cu_B), separated by $\sim 11 \text{ \AA}$.^[31] Crystallographic characterization of the oxidized form of PHM revealed a mildly activated O_2 unit in an *end-on* superoxo complex with an O–O bond distance of 1.23 \AA .^[32] The dioxygen exclusively binds to the Cu_B atom. The role of the Cu_A atom is to provide electron density to the Cu_B site for the subsequent hydroxylation pathway. Scheme 1b sketches one possible reaction pathway for the hydroxylating mechanism in PHM, as suggested by Amzel *et al.*,^[30] but other pathways were proposed, involving e.g. the oxyl radical Cu_1O formed from $\text{Cu}_1\text{S}^{\text{E}}$ species.^[11,33,34] The mechanism of the electron-transfer pathway is not completely clear, since the synthesis of model $\text{Cu}_1\text{S}^{\text{E}}$ complexes is generally hampered by their high reactivity. In some cases, the products of proton-coupled electron transfer (PCET) reactions, e.g. with TEMPOH (Scheme 1a and b, TEMPO = 2,2,6,6-tetramethylpiperidinyloxy), were isolated.^[35]



Scheme 1. a) Overview of some copper-dioxygen complexes and reaction products. b) Proposed mechanism for dioxygen activation with the enzyme PHM (adapted from Amzel *et al.* 1999, see ref. 30).

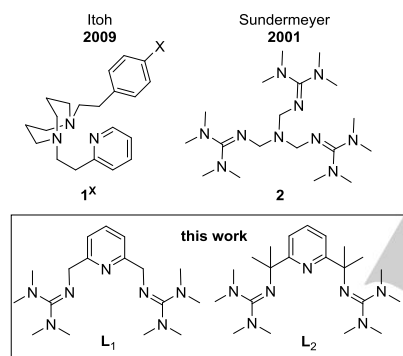
- [a] F. Schön, Dr. L. Greb, S. Leingang, Dr. E. Kaifer, Prof. H.-J. Himmel
Anorganisch-Chemisches Institut
Ruprecht-Karls-Universität Heidelberg
Im Neuenheimer Feld 270, 69120 Heidelberg, Germany
E-Mail: hans-jorg.himmel@aci.uni-heidelberg.de
http://www.uni-heidelberg.de/fakultaeten/chemgeo/aci/himmel/
- [b] F. Biebl, Dr. B. Grimm-Lebsanft, M. Teubner, Prof. M. A. Rübhausen
Institut für Nanostruktur- und Festkörperphysik
Universität Hamburg and Center for Free Electron Laser Science
Luruper Chaussee 149, 22761 Hamburg, Germany

Supporting information for this article is given via a link at the end of the document.

There are two types of hydroxylation, initiated by copper-dioxygen complexes: 1) Aromatic hydroxylation^[36] and aliphatic hydroxylation^[37] due to dinuclear oxo species which are not relevant for the above-mentioned enzymes, and 2) aliphatic hydroxylation attributable to mononuclear dioxygen complexes (Scheme 1a) as described in the following. In 2009, Itoh *et al.* reported unique examples for direct aliphatic C–H bond cleavage reactions, leading to ligand hydroxylation, as suggested for the above-mentioned enzymes, starting with

$\text{Cu}_1\text{S}^{\text{E}}$ complexes exhibiting an *N*-[2-(2-pyridyl)ethyl]-1,5-diazacyclooctane tridentate ligand (1^{X} , Scheme 2).^[38,39] Aliphatic ligand hydroxylation is also known for a $\text{Cu}_1\text{S}^{\text{E}}$ complex bearing the tris[2-(*N*-tetramethylguanidyl)-ethyl]-amine ligand (2 , Scheme 2),^[38,39] but only after the reaction with an hydrogen-atom donor (TEMPOH, phenols), or the reaction of the Cu^{I} complex with PhIO. These findings were explained by the formation of another species, a $\text{Cu}_1\text{P}^{\text{H}}$ or Cu_1O complex, which is responsible for the hydroxylating activity.^[35] There are a few more examples for Cu^{I} complexes exhibiting aliphatic ligand oxidation when exposed to dioxygen, but in all these cases a $\text{Cu}_1\text{S}^{\text{E}}$ complex could not be spectroscopically detected.^[40–43]

Moreover, a special ligand design with sterically demanding groups is required to prohibit formation of higher nuclear complexes, either as peroxy-complexes $\text{Cu}_2\text{P}^{\text{E}}$ or $\text{Cu}_2\text{P}^{\text{S}}$ ^[44,45] or as dioxy-complex Cu_2O_2 (bis(μ -oxo)-dicopper(III)).^[46] Several groups studied dioxygen binding of guanidine-copper complexes. Hence dinuclear oxo- (Cu_2O_2) and peroxy- ($\text{Cu}_2\text{P}^{\text{S}}$) complexes of bisguanidine ligands were reported.^[46,47] Especially interesting is the ability of trisguanidine-copper complexes (ligand 2 , Scheme 2) to form remarkably stable copper-superoxo complexes of type $\text{Cu}_1\text{S}^{\text{E}}$ ^[18,21] that allowed the first structural characterization of a $\text{Cu}_1\text{S}^{\text{E}}$ complex and a detailed evaluation of its reactivity.^[19,48]



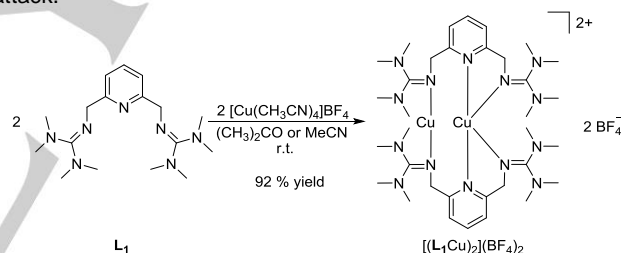
Scheme 2. Lewis structures of two previously used ligands 1^{X} ($\text{X} = \text{OMe}, \text{Me}, \text{H}, \text{Cl}, \text{NO}_2$)^[38,39] and 2 ^[49] in aliphatic ligand hydroxylation reactions via $\text{Cu}_1\text{S}^{\text{E}}$ complexes and the two bisguanidine ligands 2,6-bis(tetramethylguanidino-methyl)-pyridine (L_1) and 2,6-bis(1-tetramethyl-guanidino-1-methyl-ethyl)-pyridine (L_2) used in this work.

In the last years, our group intensively explored the chemistry of copper complexes exhibiting guanidino-substituted aromatics as ligands.^[50] We also demonstrated their use as catalysts for oxidation reactions with dioxygen.^[51] Herein we report two new copper complexes with the bisguanidine ligands L_1 and L_2 (Scheme 2). They form mononuclear copper-dioxygen species that might be interesting in the context of enzymatic aliphatic C–H bond activation. Due to the ligand design, with three *N*-donor atoms for strong coordination and steric shielding of the coordinated metal center in the binding pocket, the formation of dinuclear, oxo-bridged complexes is prohibited.

Results and Discussion

Synthesis of the copper(I) complexes

Reaction between L_1 ^[52] and tetrakis(acetonitrile)copper(I)-tetrafluoroborate, $[\text{Cu}(\text{CH}_3\text{CN})_4]\text{BF}_4$, led to the orange dinuclear complex $[(L_1\text{Cu})_2](\text{BF}_4)_2$ in a high yield of 92% (Scheme 3). The ^1H NMR spectrum displayed a doublet and a triplet signal from the pyridine ring, a singlet signal for the methylene bridge and two singlet signals for the guanidino groups. This finding can be explained by molecular dynamics, averaging the pyridine NMR signals by fast migration of the pyridine ligands from one copper atom to the other. All signals were low-field shifted with respect to the free ligand. The UV/Vis spectrum showed a strong absorption at 210 nm ($\epsilon = 27200 \text{ M}^{-1} \text{ cm}^{-1}$) together with a shoulder at 272 nm ($\epsilon = 8640 \text{ M}^{-1} \text{ cm}^{-1}$) and a weak absorption at 357 nm ($\epsilon = 883 \text{ M}^{-1} \text{ cm}^{-1}$). Figure 1a visualizes the structure of the $[(L_1\text{Cu})_2]^{2+}$ complex, as derived from X-ray diffraction on crystals grown from a $\text{CH}_3\text{CN}/\text{Et}_2\text{O}$ solution (see SI for the similar structure of crystals grown from an acetone/ Et_2O solution). Interestingly, the two Cu^{I} atoms in this complex, separated by 2.871(1) Å, are very differently coordinated. One copper atom is bound to two guanidino nitrogen atoms and in addition to the nitrogen atoms of the pyridine rings, leading to a relatively high coordination number of four. The space-filling model highlights the buried position of this copper atom in the core of the complex, leaving virtually no free space for dioxygen attack.



Scheme 3. Reaction leading to the dinuclear Cu^{I} complex $[(L_1\text{Cu})_2](\text{BF}_4)_2$.

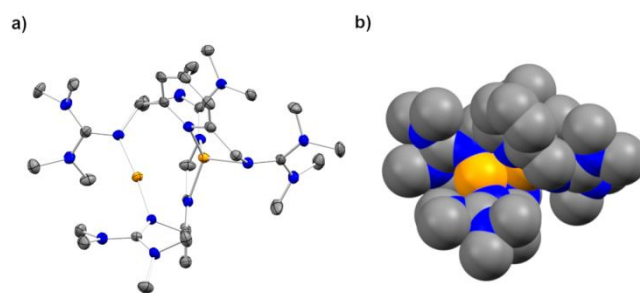


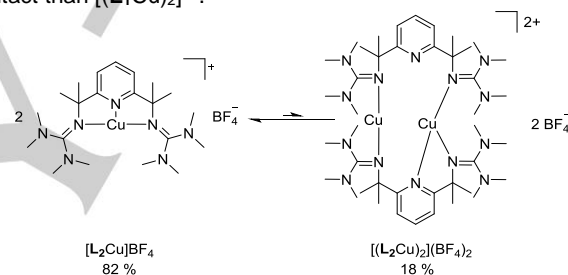
Figure 1. Structure of the complex $[(L_1\text{Cu})_2]^{2+}$ in crystals of $[(L_1\text{Cu})_2](\text{BF}_4)_2$ grown from $\text{CH}_3\text{CN}/\text{Et}_2\text{O}$ solution (Cu atoms in orange, N atoms in blue and C atoms in grey). Hydrogen atoms and counterions are omitted for clarity. The two copper atoms are separated by 2.871(1) Å (see SI for structural details). a) Structure with thermal ellipsoids (drawn at the 50% probability level). b) Space-filling model.

The second Cu^I atom exhibits a lower coordination number of two, as it is only bound to two guanidino nitrogen atoms. Consequently, this copper atom is prone for dioxygen attack (see the space-filling model in Figure 1b).

Similar IR spectra were recorded for the complex in a KBr disk and dissolved in CH₃CN, indicating that the dimeric structure is preserved in solution (see SI). ¹H DOSY NMR spectra were recorded for further assessment (see SI for details). From these experiments, the diffusion constant of the free ligand **L**₁ was estimated to 1.40·10⁻⁹ m² s⁻¹ in CD₃CN solution. With 1.01·10⁻⁹ m² s⁻¹, the diffusion constant of the copper complex obtained upon dissolving [(**L**₁Cu)₂](BF₄)₂ in CD₃CN is significantly lower, in line with the presence of a dimeric complex unit in solution. Variable-temperature ¹H NMR spectroscopy was performed to study the effect of temperature variations on the dimerization process. Although the complex revealed dynamic processes (rotation and inversion of the guanidino groups,^[53] see SI), a monomer-dimer equilibrium can be excluded. To support the experimental results, DFT calculations (TPSSH+D3/def2-TZVP) were carried out for the monomer [**L**₁Cu]⁺ and its dimer [(**L**₁Cu)₂]²⁺. The solvent effect was estimated with the conductor-like screening model (COSMO, see SI for details). The calculated structure of [(**L**₁Cu)₂]²⁺ is in very good agreement with the experimental structure. The root mean square deviation (RMSD) for the bond distances, as determined with the program aRMSD,^[54] is only 0.35 Å (see SI for details). According to these calculations, dimerization of [**L**₁Cu]⁺ is both exothermic and exergonic (Δ*H* = -182 kJ mol⁻¹ and Δ*G* = -107 kJ mol⁻¹ at 298 K, 1 bar), in full agreement with the experimental results. Hence all results confirm that the [(**L**₁Cu)₂]²⁺ units found in the solid state are preserved in solution.

Next, we synthesized the new ligand **L**₂ (see Lewis structure in Scheme 2 and experimentally derived solid-state structure in the SI) bearing methyl groups at the benzylic positions. By reaction with [Cu(CH₃CN)₄]⁺BF₄⁻, the complex [**L**₂Cu]BF₄ was obtained in 88% isolated yield. Its structural characterization in the solid state was not possible, but all experimental results point to an equilibrium between a monomeric complex [**L**₂Cu]⁺ and its dimer [(**L**₂Cu)₂]²⁺ in acetonitrile solution (Scheme 4), this time with strong preference for the monomeric complex at room temperature. From ¹H DOSY NMR spectra, a diffusion constant of 1.45·10⁻⁹ m² s⁻¹ was estimated for the free ligand **L**₂. For the copper complex, two species with significantly different diffusion constants were found. The dominating species exhibited a diffusion constant of 1.16·10⁻⁹ m² s⁻¹, and the second species a smaller one of 1.04·10⁻⁹ m² s⁻¹, being close to that of [(**L**₁Cu)₂](BF₄)₂. The obvious inference is that in CD₃CN solution a monomeric complex [**L**₂Cu]⁺ formed, together with a small amount of dimeric complex [(**L**₂Cu)₂]²⁺. This conclusion is further supported by variable-temperature ¹H NMR measurements (see SI). At high temperature (70 °C), only one species, [**L**₂Cu]⁺, was present. A weak additional set of signals appeared at room temperature, indicating the presence of small amounts of the dimer. A monomer:dimer ratio of 82:18 was estimated by signal integration. For both species, similar dynamic processes as for the [(**L**₁Cu)₂](BF₄)₂ complex were detected. At -40 °C the NMR spectra for the dimeric species [(**L**₂Cu)₂](BF₄)₂ showed an

additional signal splitting (in difference to [(**L**₁Cu)₂](BF₄)₂), arising from the formation of diastereomeric centers due to the four additional methyl groups in **L**₂. Furthermore, nuclear overhauser enhancement spectroscopy (NOESY) supported these findings by means of an exchange of signals from the guanidino groups as well as the aromatics in the major and minor product (see SI). Finally, we calculated [**L**₂Cu]⁺ and its dimer, [(**L**₂Cu)₂]²⁺, in analogy to the complexes with ligand **L**₁, and compared their energies. Surprisingly, the calculated global energy-minimum structure of [(**L**₂Cu)₂]²⁺ differed markedly from that of [(**L**₁Cu)₂]²⁺. Hence one Cu^I atom in [(**L**₂Cu)₂]²⁺ exhibits a coordination number of three, being coordinated to two guanidino nitrogen atoms and one pyridine nitrogen atom. The second Cu^I atom is coordinated to two guanidino nitrogen atoms, as in [(**L**₁Cu)₂]²⁺. Furthermore, the Cu-Cu distance (3.699 Å) is very large (for a more detailed comparison, see SI). Dimerization of [**L**₂Cu]⁺ was calculated to be mildly exothermic (Δ*H* = -42 kJ mol⁻¹) but endergonic (Δ*G* = +44 kJ mol⁻¹) at room temperature and 1 atm, in line with the experimental results. The different structures of the two complexes also led to a different chemical reactivity. Hence [**L**₂Cu]⁺ turned out to be much more sensitive to air contact than [(**L**₁Cu)₂]²⁺.



Scheme 4. Equilibrium between monomer and dimer for the complex [(**L**₂Cu)]BF₄ in acetonitrile solution, favouring the monomer at room temperature.

Reactivity of the copper(I) complex solutions toward dioxygen

Next, the reactivity of the two complexes toward dioxygen was studied. In first experiments, propionitrile solutions of [**L**₂Cu]BF₄ and [(**L**₁Cu)₂](BF₄)₂ were cooled to -80 °C and -40 °C, respectively, and the changes in the UV/Vis spectra upon addition of a pre-cooled solution of propionitrile, saturated with dioxygen, were monitored. Figure 2 visualizes the changes in the UV/Vis spectra upon dioxygen addition.

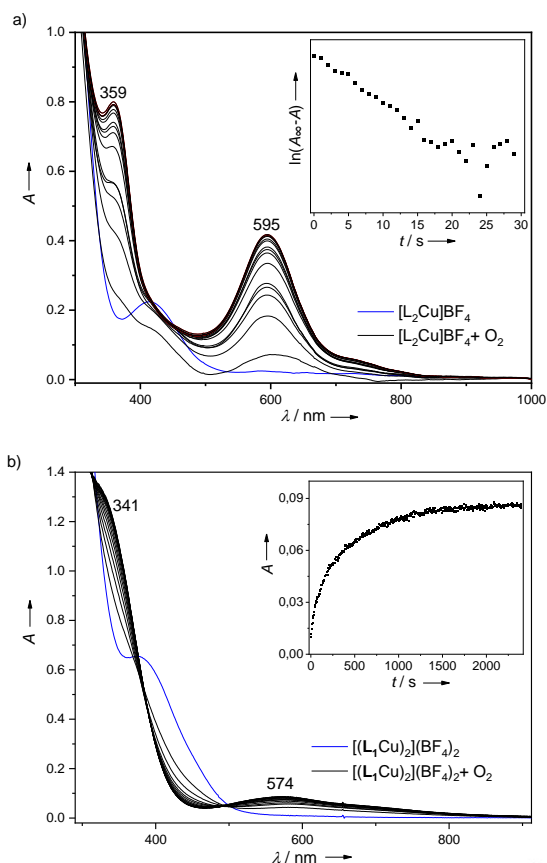


Figure 2. Spectral changes for the reaction of a) $[\text{L}_2\text{Cu}]\text{BF}_4$ ($4.34 \cdot 10^{-4} \text{ mol L}^{-1}$) for the first 30 s at -80°C (Inset: First-order plot ($\ln(A_\infty - A)$) vs. time) based on the absorbance change at 595 nm) and b) $[(\text{L}_1\text{Cu})_2](\text{BF}_4)_2$ ($2.49 \cdot 10^{-4} \text{ mol L}^{-1}$) for the first 2500 s at -40°C (Inset: Absorbance change at 574 nm) in propionitrile with dioxygen.

For the monomeric copper complex $[\text{L}_2\text{Cu}]\text{BF}_4$, a fast evolution (10 s) of intense bands at 359 nm ($\epsilon = 1800 \text{ L mol}^{-1} \text{ cm}^{-1}$) and 595 nm ($\epsilon = 970 \text{ L mol}^{-1} \text{ cm}^{-1}$) was observed which follows a first order kinetics for the reaction with dioxygen at -80°C . The wavelengths of the absorption maxima and their extinction coefficient are close to those reported previously in the literature for an *end-on* superoxo complex, $\text{Cu}_1\text{S}^{\text{E}}$.^[2,23,35] Due to its high intensity, the absorption at 595 nm clearly qualifies for a characteristic copper-dioxygen charge-transfer transition. The formation of a *side-on* superoxo complex $\text{Cu}_1\text{S}^{\text{S}}$ ^[2,25] or other dioxygen species, that typically display only weak d-d transitions in the region around 600 nm, can be excluded. The bands assigned to the $\text{Cu}_1\text{S}^{\text{E}}$ complex decreased again with time ($t_{1/2} \approx 5 \text{ min}$), indicating that the complex is unstable even at low temperature. Addition of TEMPOH produced the fast decline of the bands at 595 and 359 nm (see SI), as typical for *end-on* superoxo complexes.^[2,23,35] The Resonance Raman (rR) spectrum (excited with 329 nm light) of an oxygenated solution of $[\text{L}_2\text{Cu}]\text{BF}_4$ at -93°C included an O-isotope sensitive signal at 1136 cm^{-1} ($\Delta^{18}\text{O}_2 = 65 \text{ cm}^{-1}$; Figure 3). The peak position and associated isotope shift is similar to those reported for $\text{Cu}_1\text{S}^{\text{E}}$ complexes^[18,21,23, 55] and is assigned to the O–O stretching

vibration, supporting the formulation of an $\text{Cu}_1\text{S}^{\text{E}}$ complex. Due to the monomer-dimer equilibrium, some of the dimeric complex $[(\text{L}_2\text{Cu})_2](\text{BF}_4)_2$ should be present at the low temperature used in the experiment. However, due to a significantly higher reactivity of the monomeric complex towards dioxygen, it can be assumed that predominantly monomeric $[\text{L}_2\text{Cu}]\text{BF}_4$ reacts with dioxygen in a steady state manner, even at low temperature.

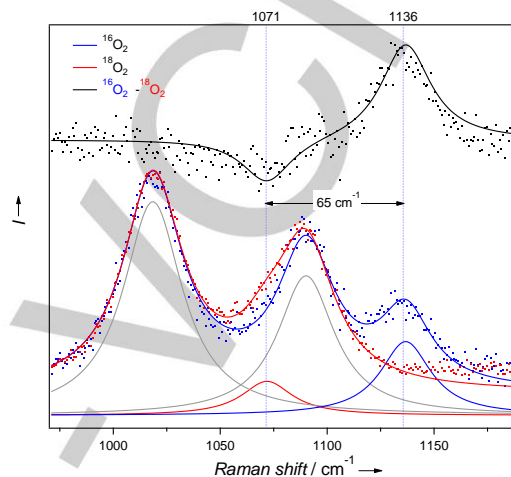
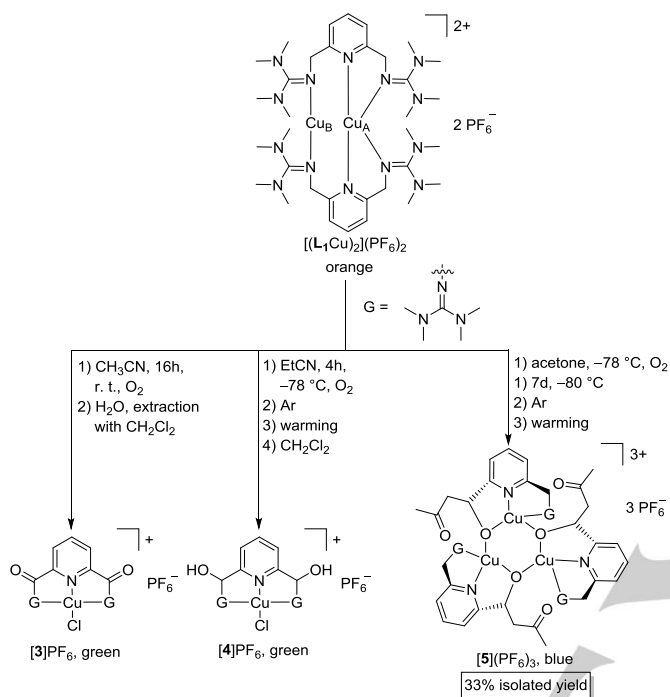


Figure 3. Resonance Raman spectra after the oxygenation of $[\text{L}_2\text{Cu}]\text{BF}_4$ with $^{16}\text{O}_2$ or $^{18}\text{O}_2$ at -93°C and difference spectrum ($^{16}\text{O}_2 - ^{18}\text{O}_2$), $\lambda_{\text{ex}} = 329 \text{ nm}$ also showing the individual Lorentzians used for fitting the data.

In the case of the dimeric complex $[(\text{L}_1\text{Cu})_2](\text{BF}_4)_2$, a much slower ($> 1500 \text{ s}$) evolution of two new bands (one at 341 nm ($\epsilon = 4900 \text{ L mol}^{-1} \text{ cm}^{-1}$) and another extremely broad one at 574 nm ($\epsilon = 345 \text{ L mol}^{-1} \text{ cm}^{-1}$)) is observed in the UV/Vis spectra upon dioxygen addition at a temperature of -40°C . No further changes were observed with time, indicating that the corresponding species is stable at -40°C . Clearly, the band at 574 nm cannot be attributed to a charge-transfer transition due to its low extinction coefficient, but rather belongs to a Cu^{II} d-d transition. UV/Vis spectra were also recorded for dioxygen addition at lower temperatures (-80°C) but gave essentially the same results. Low-temperature Raman measurements of an oxygenated solution of $[(\text{L}_1\text{Cu})_2](\text{BF}_4)_2$ at -40°C ($\lambda_{\text{ex}} = 283 \text{ nm}$) showed no O-isotope sensitive bands between 500 and 2000 cm^{-1} . On these grounds, the bands almost certainly do not belong to the initial copper-dioxygen complex, but to a rapidly formed decomposition product. The high positive charge and the steric hindrance are factors that might be relevant for the differences in the reactivity toward dioxygen between the dimeric complex $[(\text{L}_1\text{Cu})_2]^{2+}$ and the monomeric complex $[\text{L}_2\text{Cu}]^+$. Having studied the reactivity toward dioxygen at low-temperature with UV/Vis spectroscopy, we repeated the reaction for $[(\text{L}_1\text{Cu})_2]^{2+}$ on a larger scale with varying solvents and temperatures (Scheme 5). In experiments, in which the complex $[(\text{L}_1\text{Cu})_2](\text{PF}_6)_2$ was reacted with dioxygen in acetonitrile at room temperature and the reaction mixture subsequently quenched with water, complex **[3]** (Scheme 5 and Figure 4) was crystallized, after extraction with dichloromethane, from a saturated acetonitrile solution. Ligand L_1 was not only hydroxylated, but further oxidized to a diketone. In addition, a

chloride ion, abstracted from a dichloromethane solvent molecule, coordinated to the Cu^{II} atom. We repeated the reaction (Scheme 5) at -78°C and passed Ar through the reaction mixture (~ 5 min) at this low temperature to remove free (un-coordinated) dioxygen. After warming to room temperature and solvent removal in vacuo, dichloromethane was added.



Scheme 5. Formation of the mononuclear Cu^{II} complexes **[3]** PF_6 and **[4]** PF_6 , and the trinuclear Cu^{II} complex **[5]** $(\text{PF}_6)_3$ from reaction between $[(\text{L}_1\text{Cu})_2](\text{PF}_6)_2$ and dioxygen at different conditions (temperature, solvent).

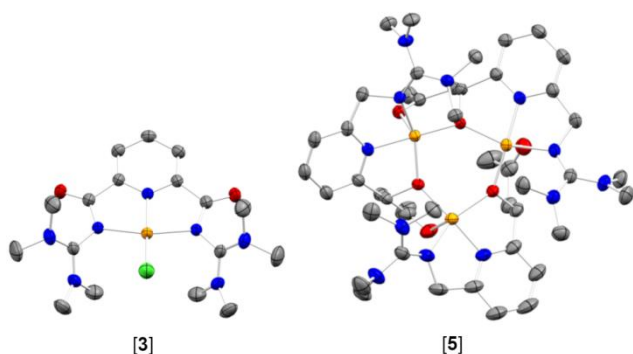


Figure 4. Structures of **[3]** PF_6 and **[5]** $(\text{PF}_6)_3$ (Cu atoms in orange, N atoms in blue, Cl atoms in green, O atoms in red and C atoms in grey). Hydrogen atoms, co-crystallized solvent molecules and counter-ions are omitted for clarity. Thermal ellipsoids are drawn at the 50% probability level (see SI for details).

The HR ESI-MS spectra of the reaction mixture displayed a peak at the mass of the doubly-hydroxylated complex **[4]** (see

Scheme 5). This finding led us to the conclusion that the oxidation to the ketone occurs in a secondary reaction after ligand hydroxylation. Now, we studied the reaction at low temperature, using acetone instead of acetonitrile as solvent. In this experiment, we injected dioxygen for ca. 5 min into a solution of the complex $[(\text{L}_1\text{Cu})_2](\text{PF}_6)_2$ in acetone at -78°C , resulting in a green-bluish mixture that was stored in the freezer (-80°C , 7 d). After purging the solution with argon (~ 5 min), warming to room temperature and overlaying with Et_2O , blue crystals of the trinuclear copper complex **[5]** were obtained in 33% isolated yield (Scheme 5 and Figure 4). The three copper atoms are coordinated by three monoanionic new ligands that result from oxidative removal of one guanidino group and further reaction with an acetone solvent molecule. A central six-membered ring of alternating copper and oxygen atoms is formed, and coordination of the guanidino group and the pyridine nitrogen atoms complete the coordination number four of each copper atom. In all three cases, an aliphatic ligand hydroxylation occurred in the first place.

Based on the accumulated experimental results it is assumed that a labile $\text{Cu}_1\text{S}^{\text{E}}$ complex is initially formed, leading to intramolecular ligand hydroxylation. The formation of higher nuclear complexes, i. e. Cu_2O_2 complexes (Scheme 1a), which are also known for hydroxylating activity, can be excluded due to the steric hindrance of $[(\text{L}_1\text{Cu})_2]^{2+}$ (with a stable dimeric structure in MeCN solutions), as illustrated in the space filling model (Figure 1), and from the results obtained with the complex $[\text{L}_2\text{Cu}](\text{BF}_4)$. Furthermore, we tested the hydroxylating activity of $[(\text{L}_2\text{Cu})\text{O}_2]\text{BF}_4$ by addition of 10 eq. of N2-benzyltetramethylguanidine (**6**) to the previously generated $\text{Cu}_1\text{S}^{\text{E}}$ complex at low temperatures in the UV/Vis. Even after warming to room temperature, no hydroxylation products of **6** were found (GC-MS). Since methylation of the ligand is not expected to have a great impact on the reactivity at the copper atom, we exclude monomeric $[(\text{L}_1\text{Cu})\text{O}_2]\text{BF}_4$ to be responsible for the hydroxylation reaction in the complexes **[3]**, **[4]** and **[5]** (Scheme 5).

Solid-state reaction of $[(\text{L}_1\text{Cu})_2](\text{BF}_4)_2$ with dioxygen

Treatment of crushed crystals of $[(\text{L}_1\text{Cu})_2](\text{BF}_4)_2$ with a mixture of $^{16}\text{O}_2$ and $^{18}\text{O}_2$ resulted in a color change from orange to green. After removal of the dioxygen with Ar, the reaction product was dissolved in dichloromethane. The HR ESI-MS analysis (Figure 5a) found peaks at m/z 441.1911 for $[\text{L}_1+\text{Cu}+\text{C}^{16}\text{O}_2\text{H}]^+$ and at m/z 443.1956 and 445.1993, due to $[\text{L}_1+\text{Cu}+\text{C}^{16}\text{O}^{18}\text{OH}]^+$ and $[\text{L}_1+\text{Cu}+\text{C}^{18}\text{O}_2\text{H}]^+$. CID experiments of the isolated ions (MS-MS) indicated the dissociation of C^{16}O_2 , $\text{C}^{16}\text{O}^{18}\text{O}$ and C^{18}O_2 , respectively, from these species, arguing for the coordination of formate to the copper complex. Control experiments without the addition of dioxygen, as well as the incorporation of the $^{18}\text{O}_2$ into the carbon dioxide, argue against the presence of impurities in the copper complex or the ESI-MS spectrometer as sources for the observed mass signals. Therefore, it is assumed that one of the tetramethylguanidino groups is hydroxylated and further oxidized to formate by the copper complex. IR spectra, recorded for KBr disks of solid $[(\text{L}_1\text{Cu})_2](\text{BF}_4)_2$ after the reaction with $^{16}\text{O}_2$

or $^{18}\text{O}_2$ displayed some differences in the region around 1600 cm^{-1} typically for $\nu(\text{C}=\text{O})$ vibrations, indicating that hydroxylation took place in the solid state. Unfortunately, the presence of strong $\nu(\text{C}=\text{N})$ vibrations of the remaining guanidino groups hampered an unambiguous assignment of the IR absorption maxima in this region (see SI).

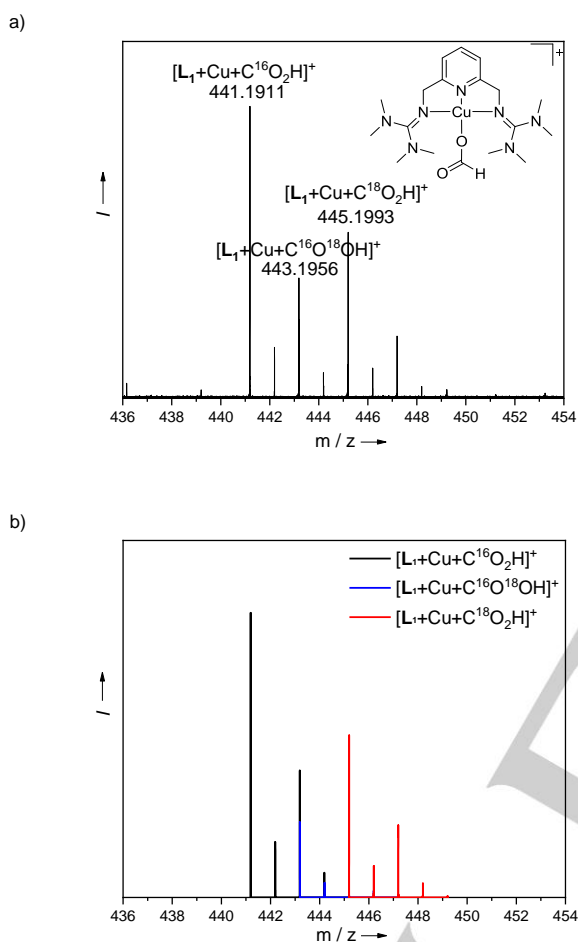


Figure 5. a) ESI-MS spectra recorded in DCM for $[(\text{L}_1\text{Cu})_2](\text{BF}_4)_2$ after solid-state reaction with a mixture of $^{18}\text{O}_2$ and $^{16}\text{O}_2$. The Lewis structure of the suggested fragment is shown in the upper right corner. b) Simulation of the fragments $[\text{L}_1+\text{Cu}+\text{C}^{16}\text{O}_2\text{H}]^+$, $[\text{L}_1+\text{Cu}+\text{C}^{16}\text{O}^{18}\text{OH}]^+$ and $[\text{L}_1+\text{Cu}+\text{C}^{18}\text{O}_2\text{H}]^+$.

DFT calculations

The structures of the two $\text{Cu}_1\text{S}^{\text{E}}$ complexes were calculated to obtain more detailed information, considering both triplet and broken-symmetry states using the TPSSH+D3 functional and the TZVP basis set. To evaluate the accuracy of our computations, we first carried out calculations for the unique example of a structurally characterized $\text{Cu}_1\text{S}^{\text{E}}$ complex (for more details, see SI), featuring the tris[2-(*N*-tetramethylguanidyl)-ethyl]amine ligand (**2**, Scheme 2).^[21] The calculated O-O bond length is 1.282 \AA , in pleasing agreement with the experimentally determined bond length of $1.280(3)\text{ \AA}$.^[21,48]

The triplet state is computed in both cases to be lower in energy (by 8.8 kJ mol^{-1} for $[\text{L}_2\text{CuO}_2]^+$ and by 22.2 kJ mol^{-1} for $[(\text{L}_1\text{Cu})_2\text{O}_2]^{2+}$) than the broken-symmetry state. Figure 6 illustrates the optimized structures for the triplet ground states of the dinuclear $[(\text{L}_1\text{Cu})_2\text{O}_2]^{2+}$ and the mononuclear $[\text{L}_2\text{CuO}_2]^+$ $\text{Cu}_1\text{S}^{\text{E}}$ complexes. The structural parameters for $[\text{L}_2\text{CuO}_2]^+$ are 1.936 and 2.734 \AA for the Cu-O distances, and 113.8° for the Cu-O-O angle. The O-O bond length of 1.300 \AA , compares with a bond length of 1.21 \AA in free dioxygen,^[56] supporting the formulation as a strongly activated superoxide. An example for a $\text{Cu}_1\text{S}^{\text{E}}$ complex with a weak degree of charge-transfer is the enzyme PHM (O-O bond length of 1.23 \AA)^[32]; whereas a strong degree of charge-transfer in $\text{Cu}_1\text{S}^{\text{E}}$ complexes results in O-O distances of ca. 1.29 \AA .^[23,57,58]

The structural parameters calculated for the dinuclear complex $[(\text{L}_1\text{Cu})_2\text{O}_2]^{2+}$ (2.254 and 3.050 \AA for the Cu-O distances, 118.2° for the Cu-O-O angle and 1.235 \AA for the O-O bond length) indicate much weaker degree of charge-transfer in the copper-dioxygen complex, nearly identical to that reported for PHM.^[32] In line with the space-filling model (Figure 1b) only one copper atom is accessible for O_2 coordination, the twofold-coordinated copper atom. The reduced ability of the copper atom in $[(\text{L}_1\text{Cu})_2\text{O}_2]^{2+}$ to donate electron density to the dioxygen unit might result from its low coordination number. A subsequent reaction to give higher nuclear complexes (see Scheme 1a) is prohibited by the steric demand of the ligand. The calculations found no other energy minima for isomeric copper-dioxygen complexes. For example, starting with a structure with a *side-on* ($\text{Cu}_1\text{S}^{\text{S}}$) bound dioxygen unit, the calculation converged to the structure of the *end-on* superoxo ($\text{Cu}_1\text{S}^{\text{E}}$) complex.

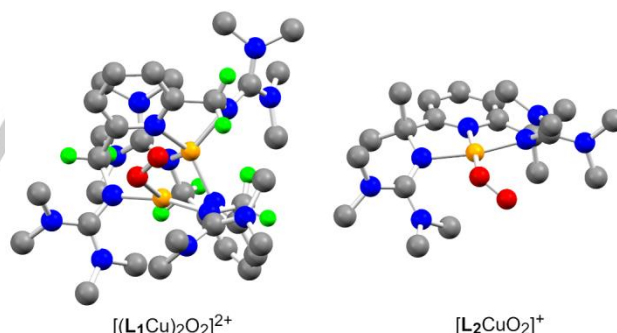


Figure 6. DFT optimized structures of *end-on* triplet Cu^{II} superoxo complexes (Cu atoms in orange, O atoms in red, N atoms in blue, C atoms in grey and H atoms from the methylene bridge ($\text{H}(\text{CH}_2)$) in green). Hydrogen atoms are omitted for clarity. The shortest Cu-O \cdots H(CH_2) distance is 3.188 \AA .

Subsequently, the low-energy electronic excitations for $[\text{L}_2\text{CuO}_2]^+$ were calculated with TD-DFT and compared with the excitations observed in the UV/Vis spectra (Figure 7a). For the monomeric complex $[\text{L}_2\text{CuO}_2]^+$, the calculations predict a single strong electronic transition in the visible region at 596 nm , involving predominantly orbitals at the Cu^{II} atom and the superoxide unit. Hence the calculations are in excellent agreement with the experimental spectrum, showing a strong band at 596 nm . To understand the hydroxylating reactivity of $[(\text{L}_1\text{Cu})_2]^{2+}$, we first examined the electronic structure of the

initially formed $\text{Cu}_1\text{S}^{\text{E}}$ complex based on DFT calculations. The spin density determined by a natural population analysis^[59] mainly resides on the two oxygen atoms (0.87 and $0.85 \text{ e} \text{ \AA}^{-3}$, respectively) due to weak charge-transfer in the copper-dioxygen complex, as indicated by the short O-O bond (1.235 \AA). As already mentioned, the low coordination number of two for the Cu_B atom (Scheme 6), and the high total charge of $2+$ of the complex could be responsible for this weak charge-transfer in the copper-dioxygen complex. The spin density at the Cu_B atom is $0.20 \text{ e} \text{ \AA}^{-3}$. Interestingly, a small but significant spin density of $0.023 \text{ e} \text{ \AA}^{-3}$ was found at the buried Cu_A atom. The existence of spin density at the fourfold coordinated Cu_A atom indicates its ability to transfer electron-density to Cu_B (see below). With $0.0076 \text{ e} \text{ \AA}^{-3}$, the total spin density at the pyridine ring is very small.

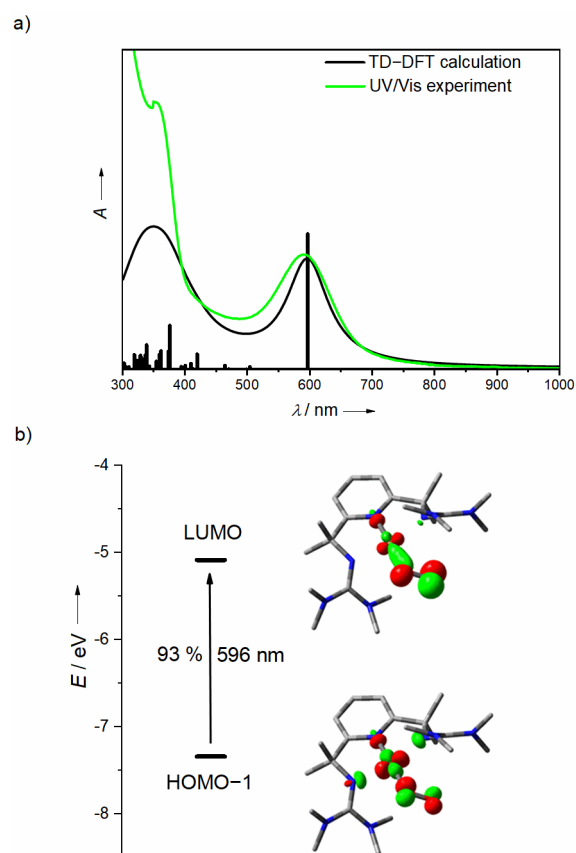


Figure 7. a) Comparison between the TD-DFT (TPSSH+D3/def2-TZVP) results for the 50 lowest-energy electronic excitations and the UV/Vis spectrum for $[\text{L}_2\text{CuO}_2]^+$. b) Isodensity plots for the orbitals involved in the low-energy (charge-transfer) transition at 596 nm.

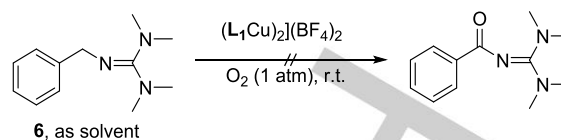
Having studied the electronic structure of the initially formed $\text{Cu}_1\text{S}^{\text{E}}$ complex, quantum-chemical calculations for the first steps in the hydroxylating mechanism were performed. According to the literature, basically three intermediates ($\text{Cu}_1\text{S}^{\text{E}}$, $\text{Cu}_1\text{P}^{\text{H}}$, Cu_1O) are considered for the hydroxylating activity of the enzyme PHM.^[11,33,34] The formation of a $\text{Cu}_1\text{P}^{\text{H}}$ complex (which

could further react to a Cu_1O species) by proton transfer from a solvent molecule to the O_2 unit of the $\text{Cu}_1\text{S}^{\text{E}}$ complex, as assumed from DFT calculations in the literature, could be excluded.^[33] The high pK_a value of acetonitrile argues against this mechanism. In all three cases ($[\mathbf{3}]\text{PF}_6$, $[\mathbf{4}]\text{PF}_6$ and $[\mathbf{5}](\text{PF}_6)_3$), intramolecular proton-coupled electron transfer (PCET, Scheme 6a) to the dioxygen unit attached to Cu_B is assumed to be the first step of the reaction sequence, in analogy to the mechanism reported by Itoh *et al.*^[39] One could identify two possible reaction sites for hydrogen atom abstraction at the methylene bridge, denoted **L** and **R** in Scheme 6a.

Hydrogen atom abstraction at the **L** reaction site can occur after rotation around the Cu-O bond, reducing the distance between the outer oxygen atom and the hydrogen atom to $\sim 3.6 \text{ \AA}$. A cooperative effect of the Cu_A center leads to a stabilization of the PCET product through delocalization of the spin density to Cu_A , as expressed by the two mesomeric structures L_I and L_{II} (Scheme 6a), and the guanidino groups. A natural population analysis indeed found spin density (Scheme 6b) not only at the activated methylene bridge ($0.52 \text{ e} \text{ \AA}^{-3}$), but also at the pyridine ring as well as at the guanidino group. In addition, the spin density at the Cu_A atom increased from $0.023 \text{ e} \text{ \AA}^{-3}$ ($[(\text{L}_I\text{Cu})_2(\text{O}_2)]^{2+}$) to $0.084 \text{ e} \text{ \AA}^{-3}$, in line with a partial oxidation of Cu_A as expressed by the Lewis structure L_{II} . The relevance of structure L_{II} is further demonstrated by a significant shortening of the bonds highlighted in orange (see Scheme 6a, for detailed comparison see SI). The calculated Gibbs free energy change (at 298.15 K, 1 atm) for the intramolecular PCET process for $[(\text{L}_I\text{Cu})_2(\text{O}_2)]^{2+}$ of 46 kJ mol^{-1} is lower than that reported by Itoh *et al.*^[39] for the analogue process in mononuclear copper complexes of ligand $\mathbf{1}^{\text{X}}$ (69 kJ mol^{-1} for $\text{X} = \text{H}$). This result demonstrates the importance of the cooperative effect of the Cu_A atom, that stabilizes the PCET product with respect to the $[(\text{L}_I\text{Cu})_2(\text{O}_2)]^{2+}$ starting complex though the resulting mesomeric stabilization of L_I and L_{II} (Scheme 6a). A transition state **TS1** was localized (see SI). The relative free activation energy of 122 kJ mol^{-1} was estimated with a single-point calculation using COSMO ($\epsilon_r = 37.50$). The hydrogen atom at reaction site **R** is closest to the superoxide oxygen with 3.188 \AA , without the need of a further rotation. In addition, the calculated free energy change (298.15 K, 1 atm) for the intramolecular PCET process is only 34 kJ mol^{-1} , being by 12 kJ mol^{-1} lower than that calculated for reaction site **L**. This can be explained by a better mesomeric stabilisation of the PCET product in R_I and R_{II} , leading to a high spin density at Cu_A of $0.13 \text{ e} \text{ \AA}^{-3}$. The spin density at Cu_B is $0.45 \text{ e} \text{ \AA}^{-3}$. Unfortunately, we were not able to find a transition state for this PCET process so that it is not clear if reaction occurs both at **R** and **L** or preferentially at one of these sites. The relatively high activation energy of 122 kJ mol^{-1} is close to that estimated for the C-H bond cleavage in the enzyme PHM.^[60] As emphasized previously, the environment plays an important role in calculating the activation barrier in this process where the experimental value should be significantly lower. Therefore, we suggest an overestimation of the activation energy especially due to the inaccuracy in calculating the solvent effect with COSMO.

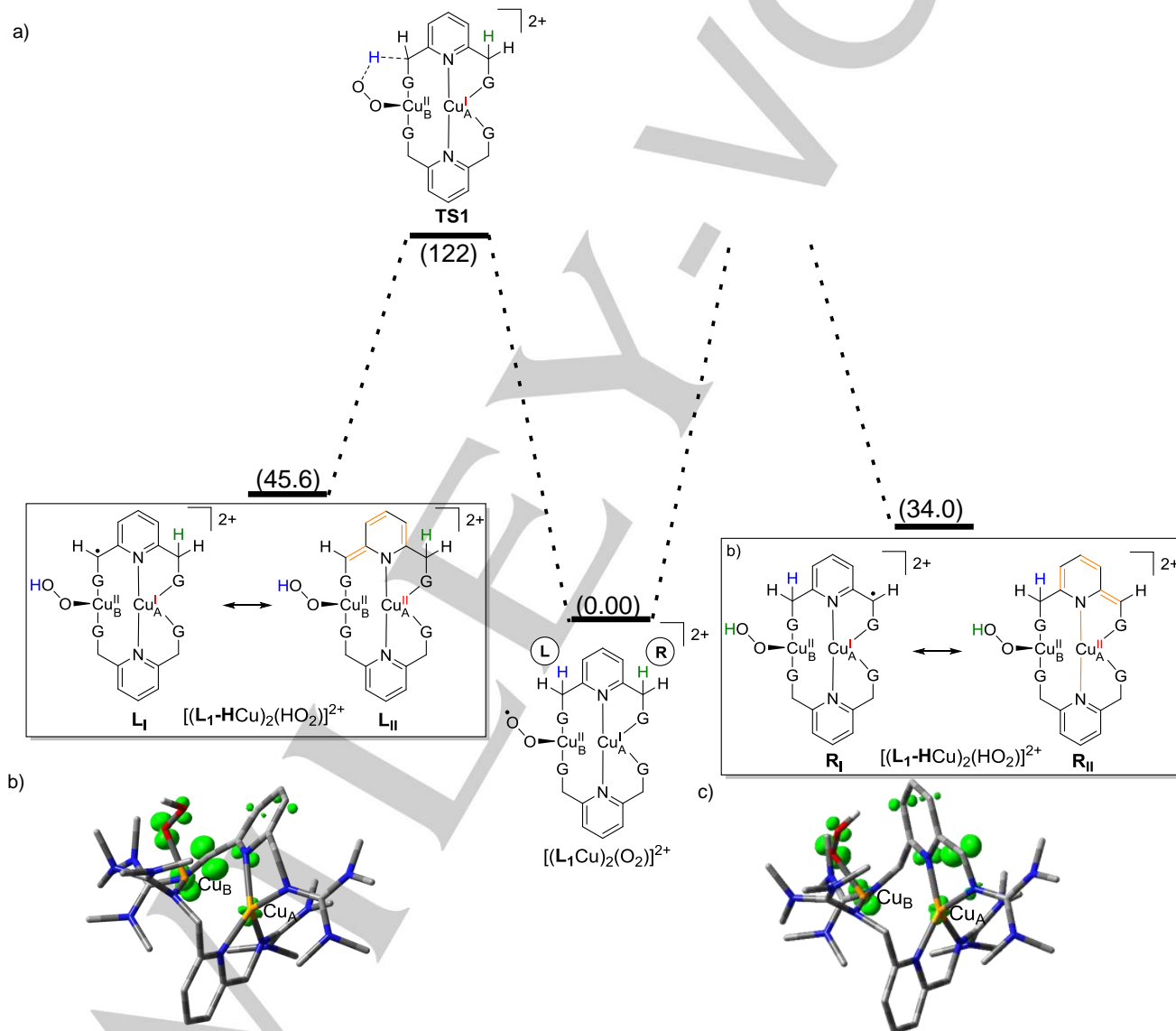
Substrate oxidation experiments

To further illuminate the role of metal cooperativity in ligand hydroxylation, we tested the hydroxylation of the external guanidine **6** with complex $[(L_1Cu)_2](PF_6)_2$ and dioxygen (Scheme 7). No reaction was observed, although the reaction was carried out in neat **6**, in accordance with the importance of metal cooperativity through the mesomeric stabilisation of **I** and **II** (Scheme 6a).



Scheme 7. Attempted hydroxylation of the external substrate **6** with $[(L_1Cu)_2](PF_6)_2$. No reaction occurred, in line with the importance of metal cooperativity for the hydroxylation of L_1 in the $[(L_1Cu)_2]^{2+}$ complex.

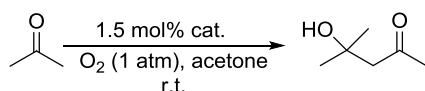
Recently, the first example of a nucleophilic copper superoxide was reported that induces a catalytic aldol reaction, i.e. with



Scheme 6. a) Energy profile (in kJ mol^{-1}) of the proposed hydroxylating pathway (two possible reaction sites **L** and **R**). Bonds of L_{II} and R_{II} highlighted in orange are shortened in comparison with $[(L_1Cu)_2(O_2)]^{2+}$. b) and c) Calculated spin density for $[(L_1Cu)_2(O_2)]^{2+}$ (green circles, TPSSH+D3/def2-TZVP), hydrogen atoms (except OH) omitted for clarity (Cu atoms in orange, N atoms in blue, O atoms in red and C atoms in grey).

acetone, forming 4-hydroxy-4-methyl-2-pentanone at room temperature.^[61] In this respect, the isolation of diacetone alcohol (4-hydroxy-4-methyl-2-pentanone, Scheme 8) as a side product in the course of the formation of **[5]** motivated us to test the two complexes $[(L_1Cu)_2](PF_6)_2$ and $[L_2CuO_2]PF_6$ in the dioxygen activation in terms of a catalytic conversion of acetone.

Both complexes were applied in catalytic amounts (1.5 mol%) and clearly showed a catalytic conversion of acetone with a turnover number (TON) of 6.50 for $[(L_1Cu)_2](PF_6)_2$ and 2.25 for the monomeric complex $[L_2Cu]PF_6$.



Scheme 8. Formation of 4-hydroxy-4-methyl-2-pentanone from acetone (cat. = $[(L_1Cu)_2](PF_6)_2$ or $[L_2CuO_2]PF_6$).

Conclusions

Herein we report on the reactions of two new copper(I) complexes, bearing bisguanidine ligands, with dioxygen. With ligand **L**₁, a dinuclear complex $[(L_1Cu)_2]^{2+}$ with two significantly different Cu^I atoms is formed, both in the solid-state and in solution. Only one of the copper atoms is able to bind dioxygen, since the other copper atom is buried inside the ligand shell. By contrast, the slightly modified ligand **L**₂ prefers formation of a mononuclear Cu^I complex $[(L_2)Cu]^+$. Both complexes are suggested to react with dioxygen to thermally labile *end-on* superoxo complexes (**Cu₁S^E**), that differ in the degree of charge-transfer. The dimeric complex $[(L_1Cu)_2(O_2)]^{2+}$ exhibits a weak degree of charge-transfer, whereas for $[(L_2)Cu(O_2)]^+$ a strong degree of charge-transfer is found.

Intramolecular hydrogen atom abstraction from the methylene bridge of **L**₁ by the O₂ unit leads to ligand hydroxylation, initiating a reaction sequence that leads (depending on the reaction conditions) either to mononuclear or trinuclear copper complexes with oxidized ligand units. With respect to the degree of charge-transfer of the copper-dioxygen complexes and the resulting C-H activation, the complex $[(L_1)Cu]^{2+}$ might be a model for the enzyme peptidylglycine α -hydroxylating monooxygenase (PHM). Further analysis showed that the two copper atoms in $[(L_1Cu)_2(O_2)]^{2+}$ communicate via charge-transfer (like for PHM and cofactor). This cooperative effect on the hydroxylating reaction between both copper atoms was further studied by DFT computations and suggested to be the key driving force for the proton-coupled electron transfer in the C-H activation process.

Furthermore, both complexes mediate acetone dimerization to 4-hydroxy-4-methyl-2-pentanone, similar to a recently reported nucleophilic **Cu₁S^E** complex.^[61,61] Studies on the reactivity of the complex $[(L_2)Cu(O_2)]^+$, which is stable for minutes at low temperatures, as a potential nucleophile are currently on the way in our laboratories.

Experimental Section

The copper complexes were stored under an inert argon atmosphere in a glovebox (MBraun Labmaster dp). All chemicals were purchased from Aldrich and used without further purification unless stated otherwise below. Solvents were dried with an MBraun Solvent Purification System, degassed by three freeze-pump-thaw cycles and stored over molecular sieves prior to their use. Propionitrile was purified and dried according to a literature procedure.^[62] Dioxygen (Air Liquide, AlphagazTM, purity $\geq 99.998\%$) was dried by passing through a short column of supported P₄O₁₀. The synthesis of **L**₁ and 2,6-bis(α -aminoisopropyl)pyridine followed literature procedures.^[62, 63] Elemental analyses were carried out at the Microanalytical Laboratory of the University of Heidelberg. NMR spectra were recorded on a Bruker Avance II 400 system (BBFO probe) or Bruker Avance III 600 spectrometer (QNP Cryoprobe, inner coil tuned to ¹³C, cold preamplifier). Prior to variable temperature measurements, the temperature was calibrated by the method of Berger *et al.*^[64] Solvent resonances were taken as references for all ¹H NMR or ¹³C NMR spectra.^[65] UV/vis spectra were recorded with a Varian Cary 5000 spectrophotometer. For IR spectroscopy, KBr disks of the compound were measured with an FTIR spectrometer (Biorad, Model Merlin Excalibur FT 3000). ESI-MS and CID experiments of isolated ions (MS-MS) relied on a Bruker ApexQe hybrid 9.4 T FT-ICR mass spectrometer. Raman measurements were performed with a UT-3 Raman spectrometer^[66], using a frequency doubled/tripled Ti:sapphire laser (Tsunami model 3960C-15HP, Spectra Physics Lasers Inc.) with a pulsewidth of 1.6-2.5 ps. The cryostat was a slightly modified version of a setup described earlier^[67] with a 1.4 ml screw cap Suprasil cuvette with septum (Hellma Analytics, Müllheim) for oxygenation, equipped with a Peltier element (QuickCool QC-127-1.4-6.0MS) and a cooling copper block which encloses three sides of the cuvette.

2,6-bis(1-tetramethylguanidino-1-methyl-ethyl)pyridine (**L**₂).

Tetramethylurea (0.9 mL, 7.4 mmol) is dissolved in chloroform (6 mL). Oxalyl chloride (3.2 mL, 37 mmol) is added dropwise, and the solution is heated to reflux (80 °C) for 18 h. Then the reaction mixture is allowed to cool back to room temperature, the solvent removed in vacuo, and the pale-yellow precipitate washed three times with portions of diethyl ether (10 mL). The colorless guanidinium chloride is dried under vacuum. 2,6-Bis(α -aminoisopropyl)pyridine (840 mg, 2.80 mmol) is dissolved in dichloromethane (20 mL), and dry triethylamine (1.7 mL, 12 mmol) is added. The chloroformamidinium chloride is dissolved again in dichloromethane (15 mL) and is subsequently added slowly to the diamine at -10 °C. The reaction mixture is stirred at -10 °C for 1 h, 10% HCl (10 mL) is added, the phases are separated, and the organic layer is washed with 10% HCl (2 x 10 mL). The combined aqueous layers are washed with dichloromethane (10 mL), and 50% KOH (20 mL) is added. Then the aqueous layer is extracted with toluene (3 x 20 mL). The combined toluene phases are dried with K₂CO₃, and the solvent is removed in vacuo to obtain a brown-coloured oil. Further purification is achieved by crystallization from an

acetonitrile solution of the oil in the freezer ($-18\text{ }^{\circ}\text{C}$) over several days. The colorless crystals are dried in vacuo to afford a colorless powder (468 mg, 120 μmol , 43%). ^1H NMR (400 MHz, CD_3CN): δ = 7.47 (m, 1 H), 7.19 (d, J = 7.8 Hz, 2 H), 2.63 (br. s, 12 H), 2.26 (br. s, 12 H), 1.50 (s, 12 H) ppm. ^{13}C NMR (100 MHz, CD_3CN): δ = 168.38, 157.41, 135.81, 60.94, 32.14 ppm. Elemental analysis (%) for $\text{C}_{21}\text{H}_{39}\text{N}_7$ (389.59): calcd. C 64.74, H 10.09, N 25.17; found C 64.38, H 9.90, N 25.25. Crystal data for L_2 : $\text{C}_{21}\text{H}_{39}\text{N}_7$, M_r = 389.59 g mol^{-1} , 0.60 mm \times 0.40 mm \times 0.30 mm, monoclinic, space group $\text{C}2/c$, lattice constants a = 24.238(5) \AA , b = 7.4070(15) \AA , c = 13.794(3) \AA , V = 2272.1(9) \AA^3 , Z = 4, d_{calc} = 1.139 g cm^{-3} , Mo $\text{K}\alpha$ radiation (graphite-monochromated, λ = 0.71073 \AA), T = 120 K, θ_{max} = 30.127 $^{\circ}$, number of reflections measured: 3326, number of independent reflections: 2224, final R indices [$I > 2\sigma(I)$]: R_1 = 0.0481, wR_2 = 0.1319.

$[(\text{L}_1\text{Cu})_2](\text{BF}_4)_2$.

A solution of tetrakis(acetonitrile)copper(I) tetrafluoroborate (94.0 mg, 299 μmol) and L_1 (100 mg, 299 μmol) in acetone (1 mL) or acetonitrile (1 mL) is stirred for 1 h at room temperature. Then the solution is overlaid with Et_2O (10 mL) to grow orange crystals overnight. The crystals are dried in vacuo to afford the product as an orange powder (110 mg, 138 μmol , 92%). ^1H NMR (600 MHz, CD_3CN): δ = 7.81 (t, J = 7.7 Hz, 1 H), 7.28 (d, J = 7.7 Hz, 2 H), 4.50 (s, 4 H), 2.79 (s, 12 H), 2.52 (s, 12 H) ppm. ^{13}C NMR (150 MHz, CD_3CN): δ = 165.85, 160.56, 139.42, 122.89, 57.83, 30.44, 39.37 ppm. Elemental analysis (%) for $\text{C}_{34}\text{H}_{62}\text{N}_{14}\text{B}_2\text{Cu}_2\text{F}_8$ (967.68): calcd. C 42.20, H 6.46, N 20.26; found C 41.82, H 6.36, N 21.02. UV/Vis (CH_3CN , c = $7.47 \cdot 10^{-5}$): λ_{max} (ϵ in $\text{L mol}^{-1} \text{cm}^{-1}$) = 210 ($2.72 \cdot 10^4$), 272 ($8.64 \cdot 10^3$), 357 (883) nm. Crystal data for $[(\text{L}_1\text{Cu})_2](\text{BF}_4)_2$: $\text{C}_{34}\text{H}_{62}\text{N}_{14}\text{B}_2\text{Cu}_2\text{F}_8$ from acetonitrile solution, M_r = 967.68 g mol^{-1} , 0.40 mm \times 0.25 mm \times 0.15 mm, triclinic, space group $P\bar{1}$, lattice constants a = 9.906(2) \AA , b = 11.162(2) \AA , c = 11.236(2) \AA , V = 1099.3(5) \AA^3 , Z = 1, d_{calc} = 1.462 g cm^{-3} , Mo $\text{K}\alpha$ radiation (graphite-monochromated, λ = 0.71073 \AA), T = 120 K, θ_{max} = 31.00 $^{\circ}$. Number of reflections measured: 13069; number of independent reflections: 10373, final R indices [$I > 2\sigma(I)$]: R_1 = 0.0505, wR_2 = 0.1364. Crystal data for $[(1\text{Cu})_2](\text{BF}_4)_2$: $\text{C}_{34}\text{H}_{62}\text{N}_{14}\text{B}_2\text{Cu}_2\text{F}_8$ from acetone solution, M_r = 967.68 g mol^{-1} , 0.80 mm \times 0.60 mm \times 0.50 mm, triclinic, space group $P\bar{1}$, lattice constants a = 16.350(3) \AA , b = 20.870(4) \AA , c = 26.131(5) \AA , V = 8917(3) \AA^3 , Z = 8, d_{calc} = 1.442 g cm^{-3} , Mo $\text{K}\alpha$ radiation (graphite-monochromated, λ = 0.71073 \AA), T = 120 K, θ_{max} = 30.063 $^{\circ}$, number of reflections measured: 13050, number of independent reflections: 8428, final R indices [$I > 2\sigma(I)$]: R_1 = 0.0541, wR_2 = 0.1792.

$[\text{L}_2\text{Cu}]\text{BF}_4$.

A solution of tetrakis(acetonitrile)copper(I) tetrafluoroborate (18.4 mg, 58.5 μmol) and L_2 (23.4 mg, 58.5 μmol) in CH_3CN (2 mL) is stirred for a period of 1 h at room temperature. Then the solvent is removed in vacuo, the residue is washed with Et_2O (2 \times 2 mL) and the solid is dried in vacuo to afford the product as an orange powder (25.0 mg, 51.7 μmol , 88%). ^1H NMR (600 MHz, CD_3CN) for the monomer: δ = 7.72 (m, 1 H), 7.30 (m, 2 H),

2.72 (s, 12 H), 2.40 (s, 12 H), 1.61 (s, 12 H) ppm; ^{13}C NMR (150 MHz, CD_3CN): δ = 167.27, 160.75, 138.37, 117.19, 62.21, 40.32, 39.45, 29.67 ppm. Elemental analysis (%) for $\text{C}_{21}\text{H}_{39}\text{N}_7\text{BCuF}_4$ (539.94): calcd. C 46.71, H 7.28, N 18.16; found C 46.73, H 7.31, N 19.09. UV/Vis (CH_3CN , c = $6.00 \cdot 10^{-5}$): λ_{max} (ϵ in $\text{L mol}^{-1} \text{cm}^{-1}$) = 212 ($3.76 \cdot 10^4$), 263 ($1.44 \cdot 10^4$), 414 (686) nm.

$[\text{3}]\text{PF}_6$.

A solution of tetrakis(acetonitrile)copper(I) hexafluorophosphate (112 mg, 299 μmol) and L_1 (100 mg, 299 μmol) in acetonitrile (1.5 mL) is stirred for a period of 1 h at room temperature. Dioxxygen is introduced via a syringe (1 bar overpressure) and the mixture is stirred for 16 h. Then water (10 mL) is added and the mixture is extracted with dichloromethane (4 \times 7 mL). The combined organic layers are dried over magnesium sulfate and the solvent is removed in vacuo. Green crystals of $[\text{3}]\text{PF}_6$ are grown from slowly evaporating a saturated acetonitrile solution. Crystal data for $[\text{3}]\text{PF}_6$: $\text{C}_{17}\text{H}_{27}\text{N}_7\text{CuO}_2\text{ClF}_6\text{P}$, M_r = 605.41 g mol^{-1} , 0.50 mm \times 0.50 mm \times 0.3 mm, orthorhombic, space group $Pnma$, lattice constants a = 11.674(2) \AA , b = 14.092(2) \AA , c = 15.341(3) \AA , V = 2523.7(9) \AA^3 , Z = 4, d_{calc} = 1.593 g cm^{-3} , Mo $\text{K}\alpha$ radiation (graphite-monochromated, λ = 0.71073 \AA), T = 120 K, θ_{max} = 30.078 $^{\circ}$, number of reflections measured: 3836, number of independent reflections: 2754, final R indices [$I > 2\sigma(I)$]: R_1 = 0.0547, wR_2 = 0.1595. HRMS (ESI+): m/z calcd for $\text{C}_{17}\text{H}_{27}\text{N}_7\text{O}_2\text{CuCl}$ [M^+] 459.1211, found 459.1213.

$[\text{4}]\text{PF}_6$.

A solution of tetrakis(acetonitrile)copper(I) hexafluorophosphate (56.0 mg, 150 μmol) and L_1 (50.0 mg, 150 μmol) in propionitrile (2 mL) is stirred for a period of 1 h at room temperature. The reaction mixture is cooled to $-78\text{ }^{\circ}\text{C}$, dioxxygen is introduced via a syringe (0.2 bar overpressure) and the mixture is stirred for 4 h. After purging the resulting blue solution with argon (~ 5 min) and warming up to room temperature (color change to green), the solvent is removed in vacuo and dichloromethane is added. HRMS (ESI+): m/z calcd for $\text{C}_{17}\text{H}_{31}\text{N}_7\text{O}_2\text{CuCl}$ [M^+] 463.1524, found 463.1525.

$[\text{5}](\text{PF}_6)_3$.

A solution of tetrakis(acetonitrile)copper(I) hexafluorophosphate (112 mg, 299 μmol) and L_1 (100 mg, 299 μmol) in acetone (3 mL) is stirred for 1 h at room temperature. Dioxxygen is introduced via a syringe ($-78\text{ }^{\circ}\text{C}$) and the mixture filtered via a syringe filter. The solution is stored for 1 week in the freezer ($-80\text{ }^{\circ}\text{C}$). Residual dioxxygen is removed by bubbling Ar (~ 5 min) through the reaction solution at $-78\text{ }^{\circ}\text{C}$. Blue crystals are grown by ether diffusion into the solution at $-18\text{ }^{\circ}\text{C}$ and washed with cold acetone (2 mL) and diethylether (5 mL). The crystals are dried in vacuo to afford $[\text{5}](\text{PF}_6)_3$ as a blue powder (50 mg, 33.3 μmol) in 33% isolated yield. Elemental analysis (%) for $\text{C}_{45}\text{H}_{69}\text{N}_{12}\text{Cu}_3\text{O}_6(\text{F}_6\text{P})_3(\text{C}_3\text{H}_6\text{O})_{1.5}$ (1543.21): calcd. C 36.78, H 4.80, N 10.89; found C 37.61, H 5.12, N 10.76. IR (KBr): ν = 3102 (w), 2009 (w), 2947 (m), 2900 (m), 2812 (w), 1698 (s), 1611 (m), 1588 (s), 1477 (m), 1427 (m), 1400 (m), 1358 (m), 1339 (w), 1294 (w), 1255 (w) 1236 (w), 1166 (s), 1146 (w), 1115(w), 1070 (m), 1054 (s), 1015 (w), 972 (w), 939 (w), 912 (m),

877 (m), 841 (s), 791 (m), 764 (m), 784 (w) 691 (m), 669 (w), 648 (m) 622 (m), 558 (s), 530 (w), 496 (m), 465 (w), 450 (w), 428 (w), 421 (m) cm^{-1} . UV/Vis (CH_3CN), $c = 4.61 \cdot 10^{-5}$: λ_{max} (ϵ in $\text{L mol}^{-1} \text{cm}^{-1}$) = 218 ($5.46 \cdot 10^4$), 267 ($2.08 \cdot 10^4$), 334 ($4.12 \cdot 10^3$), 336 ($3.03 \cdot 10^3$) nm. Crystal data for **[5](PF₆)₃**: $\text{C}_{45}\text{H}_{69}\text{N}_{12}\text{Cu}_3\text{O}_6(\text{F}_6\text{P})_3(\text{C}_3\text{H}_6\text{O})_{1.5}$, $M_r = 1543.21 \text{ g mol}^{-1}$, 0.40 mm \times 0.30 mm \times 0.15 mm, monoclinic, space group $C2/c$, lattice constants $a = 23.840(5) \text{ \AA}$, $b = 15.796(3) \text{ \AA}$, $c = 37.282(8) \text{ \AA}$, $V = 13543(5) \text{ \AA}^3$, $Z = 8$, $d_{\text{calc}} = 1.514 \text{ g cm}^{-3}$, Mo K_{α} radiation (graphite-monochromated, $\lambda = 0.71073 \text{ \AA}$), $T = 120 \text{ K}$, $\theta_{\text{max}} = 29.182^\circ$, number of reflections measured: 18224, number of independent reflections: 14550, final R indices [$I > 2\sigma(I)$]: $R_1 = 0.0567$, $wR_2 = 0.1718$.

Catalytic coupling of acetone to 4-hydroxy-4-methyl-2-pentanone

A solution of tetrakis(acetonitrile)copper(I) hexafluorophosphate (112 mg, 299 μmol) and the ligand (**L**₁ or **L**₂, see Table 1) in acetone (1.5 mL, 20 mmol) is stirred for 1 h at room temperature. Dioxygen is introduced via a syringe (1 bar overpressure) and the mixture is stirred for 20 h. 4-Hydroxy-4-methyl-2-pentanone and acetone are separated by distillation from the residue. ¹H and ¹³C NMR data are in line with those reported previously.^[68]

Table 1. Yield and weighting.

	L ₁ (100 mg, 299 μmol)	L ₂ (117 mg, 299 μmol)
Yield diacetone alcohol	114 mg, 877 μmol , TON 6.50).	77.9 mg, 671 μmol , TON 2.25)

Note: The blank experiment with ligand alone did not lead to conversion of acetone.

Raman-measurements

The laser beam was widened with a spatial filter and then focused on the cuvette inside the cryostat. The focus spot size was around 20 μm in diameter. Raman scattered light was captured with the entrance optics of the UT-3 triple monochromator spectrometer.^[66] The precursor with a concentration of 30 mmol/L in propionitrile was cooled in the cuvette cryostat to the desired temperature. Dioxygen was added via a cannula through the septum (0.02 bar overpressure for 30 sec) until a distinct color change was observed. Afterwards the solvent was immediately frozen by cooling to $-100 \text{ }^\circ\text{C}$. The used laser power in front of the entrance optics was 10.7 mW. Data was accumulated for 3x300 s and corrected for the spectral sensitivity of the instrument.

X-ray crystallographic study

Suitable crystals for single-crystal structure determination were taken directly from the mother liquor, taken up in perfluorinated polyether oil and fixed on a cryo loop. Full shells of intensity data were collected at low temperature with a Nonius Kappa CCD diffractometer (Mo-K α radiation, sealed X-ray tube, graphite monochromator). The data were processed with the standard

Nonius software.^[69] Multiscan absorption correction was applied to all intensity data using the SADABS program.^[70] The structures were solved and refined using the SHELXTL software package (Version 2014/6 and 2018/3).^[71,72] Graphical handling of the structural data during solution and refinement were performed with XPLA and OLEX2.^[73] All non-hydrogen atoms were given anisotropic displacement parameters. Hydrogen atoms were generally input at calculated positions and refined with a riding model. Due to severe disorder electron density attributed to solvent of crystallization (acetone) was removed from the structure of **[5](PF₆)₃** with the BYPASS procedure,^[74] as implemented in PLATON (squeeze/hybrid).^[75] Partial structure factors from the solvent masks were included in the refinement as separate contributions to F_{calc} . CCDC 1867620 (**L**₂), CCDC 1867616 (**[L**₁Cu)₂(BF₄)₂) from acetonitrile solution, CCDC 1867618 (**[L**₁Cu)₂(BF₄)₂) from acetone solution, CCDC 1867617 (**[5](PF₆)₃**), CCDC 1867619 (**[3](PF₆)₃**) contain the supplementary crystallographic data for this paper. These data can be obtained free of charge from The Cambridge Crystallographic Data Centre via https://www.ccdc.cam.ac.uk/data_request/cif.

Acknowledgements

The authors gratefully acknowledge continuous financial support by the *Deutsche Forschungsgemeinschaft* (DFG). The authors are grateful for the computational resources provided by the bwForCluster JUSTUS, funded by the Ministry of Science, Research and Arts and the Universities of the State of Baden-Württemberg, Germany, within the framework program bwHPC-C5. We thank Dr. J. Gross for the support with ESI-MS spectrometry.

Keywords: copper • dioxygen complexes • C–H activation • oxidation • cooperative effects

- [1] Copper-oxygen chemistry, Ed. K. D. Karlin, S. Itoh, Vol. 4 of Wiley Series on reactive intermediates in chemistry and biology, **2011**, John Wiley & Sons, Inc.
- [2] L. M. Mirica, X. Ottenwaelter, T. D. P. Stack, *Chem. Rev.* **2004**, *104*, 1013–1045.
- [3] S. Schindler, *Eur. J. Inorg. Chem.* **2000**, 2311–2326.
- [4] A. Bhagi-Damodaran, M. A. Michael, Q. Zhu, J. Reed, B. A. Sandoval, E. N. Mirts, S. Chakraborty, P. Moëne-Loccoz, Y. Zhang, Y. Lu, *Nat. Chem.* **2017**, *9*, 257–263.
- [5] S. Itoh, *Acc. Chem. Res.* **2015**, *48*, 2066–2074.
- [6] C. J. Cramer, W. B. Tolman, *Acc. Chem. Res.* **2007**, *40*, 601–608.
- [7] S. Fukusumi, K. D. Karlin, *Coord. Chem. Rev.* **2013**, *257*, 187–195.
- [8] E. I. Solomon, D. E. Heppner, E. M. Johnston, J. W. Ginsbach, J. Cicera, M. Quayyum, M. T. Kieber-Emmons, C. H. Kjaergaard, R. G. Hadt, L. Tan, *Chem. Rev.* **2014**, *114*, 3659–3853.
- [9] E. I. Solomon, D. E. Heppner, E. M. Johnston, J. W. Ginsbach, J. Cirera, M. Qayyum, M. T. Kieber-Emmons, C. H. Kjaergaard, R. G. Hadt, L. Tian, *Chem. Rev.* **2014**, *114*, 3659–3853.
- [10] J. B. Klinman, *Chem. Rev.* **1996**, *96*, 2541–2561.

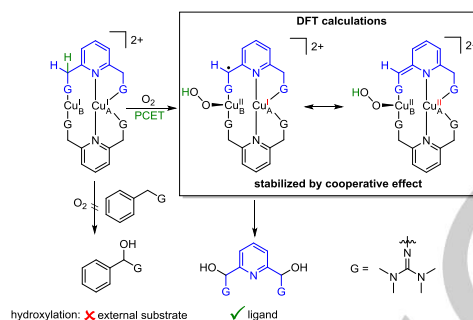
- [11] M. Rolff, F. Tuczek, *Angew. Chem.* **2008**, *120*, 2378-2381; *Angew. Chem. Int. Ed.* **2008**, *47*, 2344-2347.
- [12] I. A. Koval, P. Gamez, C. Belle, K. Selmececi, J. Reedijk, *Chem. Soc. Rev.* **2006**, *35*, 814-840.
- [13] V. Mahadevan, R.J.M.K. Gebbink, T.D.P. Stack, *Curr. Opin. Chem. Biol.* **2000**, *4*, 228-234.
- [14] M. Rolff, J. Schottenheim, G. Peters, F. Tuczek, *Angew. Chem.* **2010**, *122*, 6583-6587; *Angew. Chem. Int. Ed.* **2010**, *49*, 6438-6442.
- [15] R. E. Cowley, J. Cirera, M. F. Qayyum, D. Rokhsana, B. Hedman, K. O. Hodgson, D. M. Dooley, E. I. Solomon, *J. Am. Chem. Soc.* **2016**, *138*, 13219-13229.
- [16] E. Solem, F. Tuczek, H. Decker, *Angew. Chem.* **2016**, *128*, 2934-2938; *Angew. Chem. Int. Ed.* **2016**, *55*, 2884-2888.
- [17] M. Rolff, J. Schottenheim, H. Decker, F. Tuczek, *Chem. Soc. Rev.* **2011**, *40*, 4077-4098.
- [18] M. Schatz, V. Raab, S. P. Foxon, G. Brehm, S. Schneider, M. Reiher, M. C. Holthausen, J. Sundermeyer, S. Schindler, *Angew. Chem.* **2004**, *116*, 4460-4464; *Angew. Chem. Int. Ed.* **2004**, *33*, 4360-4363.
- [19] D. Maiti, H. C. Fry, J. S. Woertink, M. A. Vance, E. I. Solomon, K. D. Karlin, *J. Am. Chem. Soc.* **2007**, *129*, 264-265.
- [20] A. Kunishita, M. Kubo, H. Sugimoto, T. Ogura, K. Sato, T. Takui, S. Itoh, *J. Am. Chem. Soc.* **2009**, *131*, 2788-2789.
- [21] C. Würtele, E. Gaoutchenova, K. Harms, M. C. Holthausen, J. Sundermeyer, S. Schindler, *Angew. Chem.* **2006**, *118*, 3951-3954; *Angew. Chem. Int. Ed.* **2006**, *23*, 3867-3869.
- [22] M. P. Lanci, V.V. Smirnov, C.J. Cramer, E. V. Gauchenova, J. Sundermeyer, J. P. Roth, *J. Am. Chem. Soc.* **2007**, *129*, 14697-14709.
- [23] P. J. Donoghue, A. K. Gupta, D. W. Boyce, C. J. Cramer, W. B. Tolman, *J. Am. Chem. Soc.* **2010**, *132*, 15869-15871.
- [24] K. Fukisawa, M. Tanaka, Y. Moro-oka, N. Kitajima, *J. Am. Chem. Soc.* **1994**, *116*, 12079-12080.
- [25] P. Chen, D. E. Root, C. Campochiano, K. Fujisawa, E. I. Solomon, *J. Am. Chem. Soc.* **2003**, *125*, 466-471.
- [26] D. J. E. Spencer, N. W. Aboeella, A. M. Reynolds, P. L. Holland, W. B. Tolman, *J. Am. Chem. Soc.* **2002**, *124*, 2108-2109.
- [27] N. W. Aboeella, E. A. Lewis, A. M. Reynolds, W. W. Brennessel, C. J. Cramer, W. B. Tolman, *J. Am. Chem. Soc.* **2002**, *124*, 10660-10661.
- [28] A. M. Reynolds, B. F. Gherman, C. J. Cramer, W. B. Tolman, *Inorg. Chem.* **2005**, *44*, 6989-6997.
- [29] For some examples, see: a) S. T. Prigge, R. E. Mains, B. A. Eipper, L. M. Amzel, *Cell. Mol. Life Sci.* **2000**, *57*, 1236-1259. b) W. A. Francisco, G. Wille, A. J. Smith, D. J. Merkler, J. P. Klinman, *J. Am. Chem. Soc.* **2004**, *126*, 13168-13169. c) P. Chen, E. I. Solomon, *J. Am. Chem. Soc.* **2004**, *126*, 4991-5000; d) J. P. Klinman, *J. Biol. Chem.* **2006**, *281*, 3013-3016.
- [30] S. T. Prigge, A. S. Kolhekar, B. A. Eipper, R. E. Mains, L. M. Amzel, *Nat. Struct. Biol.* **1999**, *6*, 976-983.
- [31] S. T. Prigge, A. S. Kolhekar, B. A. Eipper, R. E. Mains, L. M. Amzel, *Science* **1997**, *278*, 1300-1305.
- [32] S. T. Prigge, B. A. Eipper, R. E. Mains, L. M. Amzel, *Science* **2004**, *304*, 864-867.
- [33] B. N. Sánchez-Eguía, M. Flores-Alamo, M. Orio, I. Castillo, *Chem. Comm.* **2015**, *51*, 11134-11137
- [34] A. Crespo, M. A. Martí, A. E. Røitberg, L. M. Amzel, D. A. Estrin, *J. Am. Chem. Soc.* **2006**, *128*, 12817-12828.
- [35] D. Maiti, D.-H. Lee, K. Gaoutchenova, C. Würtele, M. C. Holthausen, A. A. Sarjeant, J. Sundermeyer, S. Schindler, K. D. Karlin, *Angew. Chem.* **2008**, *120*, 88-91; *Angew. Chem. Int. Ed.* **2008**, *47*, 82-85.
- [36] For some examples, see: a) B. Herzigkeit, B. M. Flöser, T. A. Engesser, C. Näther, F. Tuczek, *Eur. J. Inorg. Chem.* **2018**, 3058-3069; b) J. Becker, Y. Y. Zhyhadlo, E. D. Butova, A. A. Fokin, P. R. Schreiner, M. Förster, M. C. Holthausen, P. Specht, S. Schindler, *Chem. Eur. J.* **2018**, *24*, 1-8; c) C. Würtele, O. Sander, V. Lutz, T. Waitz, F. Tuczek, S. Schindler, *J. Am. Chem. Soc.* **2009**, *131*, 7544-7545. d) S. Herres, A. J. Heuwing, U. Flörke, J. Schneider, G. Henkel, *Inorg. Chim. Acta.* **2005**, *358*, 1089-1095; e) S. Itoh, M. Taki, H. Nakao, P. L. Holland, W. B. Tolman, Jr. L. Que, S. Fukuzumi, *Angew. Chem.* **2000**, *17*, 409-411; *Angew. Chem. Int. Ed.* **2000**, *39*, 398-400; f) P. Comba, S. Knoppe, B. Martin, G. Rajaraman, C. Rolli, B. Shapiro, T. Sork, *Chem. Eur. J.* **2008**, *14*, 344-357; g) A. Arnold, R. Metzinger, C. Limberg, *Chem. Eur. J.* **2015**, *21*, 1198-1207; h) S. Palavicini, A. Granata, E. Monzani, L. Casella, *J. Am. Chem. Soc.* **2005**, *127*, 18031-18036.
- [37] For some examples, see: a) O. Sander, A. Henss, C. Näther, C. Würtele, M. C. Holthausen, S. Schindler, F. Tuczek, *Chem. Eur. J.* **2008**, *14*, 9714-9729. b) T. Matsumoto, H. Furutachi, S. Nagatomo, T. Tosha, S. Fujinami, T. Kitagawa, M. Suzuki, *J. Organomet. Chem.* **2007**, *692*, 111-121.; c) A. Kunushita, J. Teraoka, J. D. Scanlon, T. Matsumoto, M. Suzuki, C. J. Cramer, S. Itoh, *J. Am. Chem. Soc.* **2007**, *129*, 7248-7249. d) K. D. Karlin, P. L. Dahlstrom, S. N. Cozzette, P. M. Scensny, J. Zubieta, *J. Chem. Soc., Chem. Comm.* **1981**, 881-882; e) T.-D. J. Stumpf, M. Steinbach, C. Würtele, J. Becker, S. Becker, R. Fröhlich, R. Göttlich, S. Schindler, *Eur. J. Inorg. Chem.* **2017**, *37*, 4246-4258; f) H. R. Lucas, L. Li, A. A. N. Sarjeant, M. A. Vance, E. I. Solomon, K. D. Karlin, *J. Am. Chem. Soc.* **2009**, *131*, 3230-3245.
- [38] A. Kunushita, M. Kubo, H. Sugimoto, T. Ogura, K. Sato, T. Takui, S. Itoh, *J. Am. Chem. Soc.* **2009**, *131*, 2788-2789.
- [39] A. Kunishita, M. Z. Ertem, Y. Okubo, T. Tano, H. Sugimoto, K. Ohkubo, N. Fujieda, S. Fukuzumi, C. J. Cramer, S. Itoh, *Inorg. Chem.* **2012**, *51*, 9465-9480.
- [40] G. Izzet, J. Zeitouny, H. Akdas-Killig, Y. Frapart, S. Ménage, B. Doucziech, J. Jabin, Y. Le Mest, O. Renaud, *J. Am. Chem. Soc.* **2008**, *130*, 9514-9523.
- [41] G. Thiabaud, G. Guillemot, I. Schmitz-Afonso, B. Colasson, O. Renaud, *Angew. Chem.* **2009**, *121*, 7519-7522; *Angew. Chem. Int. Ed.* **2009**, *48*, 7383-7386.
- [42] T. Fujii, S. Yamaguchi, Y. Funahashi, T. Ozawa, T. Tosha, T. Kitagawa, H. Masuda, *Chem. Comm.* **2006**, 4428-4430
- [43] T. Fujii, S. Yamaguchi, S. Hirota, H. Masuda, *Dalton. Trans.* **2008**, 164-170.
- [44] S. Itoh, H. Kumei, M. Taki, S. Nagatomo, T. Kitagawa, S. Fukuzumi, *J. Am. Chem. Soc.* **2001**, *123*, 6708-6709.
- [45] T. Osako, K. Ohkubo, M. Taki, Y. Tachi, S. Fukuzumi, S. Itoh, *J. Am. Chem. Soc.* **2003**, *125*, 11027-11033.
- [46] For some examples, see: a) S. Herres-Pawlis, U. Flörke, G. Henkel, *Eur. J. Inorg. Chem.* **2005**, 3815-3824; b) S. Herres-Pawlis, P. Verma, R. Haase, P. Kang, C. T. Lyons, E. C. Wasinger, U. Flörke, G. Henkel, T. D. P. Stack, *J. Am. Chem. Soc.* **2009**, *131*, 1154-1169; c) V. Mahadevan, Z. Hou, A. P. Cole, D. E. Root, T. K. Lal, E. I. Solomon, T. D. P. Stack, *J. Am. Chem. Soc.* **1997**, *119*, 11996-11997; d) J. A. Halfen, S. Mahapatra, E. C. Wilkinson, S. Kaderli, V. G. Young, Jr., L. Que Jr., A. D. Zuberbühler, W. B. Tolman, *Science* **1996**, *271*, 1397-1400; e) A. Walli, S. Dechert, M. Bauer, S. Demeshko, F. Meyer, *Eur. J. Inorg. Chem.* **2014**, 4660-4676.
- [47] D. Petrovic, L. M. R. Hill, P. G. Jones, W. B. Tolman, M. Tamm, *Dalton Trans.* **2008**, 887-894.
- [48] D. Maiti, D.-H. Lee, K. Gaoutchenova, C. Würtele, M. C. Holthausen, A. A. Sarjeant, J. Sundermeyer, S. Schindler, K. D. Karlin, *Angew. Chem.* **2008**, *120*, 88-91; *Angew. Chem. Int. Ed.* **2008**, *47*, 82-85.
- [49] V. Raab, J. Kipke, O. Burghaus, J. Sundermeyer, *Inorg. Chem.* **2001**, *40*, 6964-6971.
- [50] For some recent examples, see: a) D. F. Schrempf, S. Leingang, M. Schnurr, E. Kaifer, H. Wadepohl, H.-J. Himmel, *Chem. Eur. J.* **2017**, *23*, 13607-13611; b) D. F. Schrempf, E. Schneider, E. Kaifer, H. Wadepohl, H.-J. Himmel, *Chem. Eur. J.* **2017**, *23*, 11636-11648; c) H. Herrmann, E. Kaifer, H.-J. Himmel, *Chem. Eur. J.* **2017**, *23*, 5520-

- 5528; d) D. F. Schrempf, E. Kaifer, H. Wadepohl, H.-J. Himmel, *Chem. Eur. J.* **2016**, *22*, 16187–16199; e) S. Wiesner, A. Wagner, E. Kaifer, H.-J. Himmel, *Chem. Eur. J.* **2016**, *22*, 10438–10445; f) S. Wiesner, A. Wagner, O. Hübner, E. Kaifer, H.-J. Himmel, *Chem. Eur. J.* **2015**, *21*, 16494–16503; g) A. Ziesak, T. Wesp, O. Hübner, E. Kaifer, H. Wadepohl, H.-J. Himmel, *Dalton Trans.* **2015**, *44*, 19111–19125.
- [51] F. Schön, E. Kaifer, H.-J. Himmel, *Chem. Eur. J.* **2019**, DOI: 10.1002/chem.201900583.
- [52] P. Roquette, C. König, O. Hübner, N. Wagner, E. Kaifer, M. Enders, H.-J. Himmel, *Eur. J. Inorg. Chem.* **2010**, 4770–4782.
- [53] a) V. Raab, J. Kipke, R. M. Gschwind, J. Sundermeyer, *Chem. Eur. J.* **2002**, *8*, 1682–1693; b) U. Wild, O. Hübner, A. Maronna, M. Enders, E. Kaifer, H. Wadepohl, H.-J. Himmel, *Eur. J. Inorg. Chem.* **2008**, 4440–4447; c) M. Reinmuth, U. Wild, E. Kaifer, M. Enders, H. Wadepohl, H.-J. Himmel, *Eur. J. Inorg. Chem.* **2009**, 4795–4808; d) M. Reinmuth, C. Neuhäuser, P. Walter, M. Enders, E. Kaifer, H.-J. Himmel, *Eur. J. Inorg. Chem.* **2011**, 83–90; e) P. Roquette, A. Maronna, M. Reinmuth, E. Kaifer, M. Enders, H.-J. Himmel, *Inorg. Chem.* **2011**, *50*, 1942–1955.
- [54] A. Wagner, H.-J. Himmel, *J. Chem. Inf. Model* **2017**, *57*, 428–438.
- [55] M. Weitzer, S. Schindler, G. Brehm, S. Schneider, E. Hormann, B. Jung, S. Kaderli, A. D. Zuberbühler, *Inorg. Chem.* **2003**, *42*, 1800.
- [56] Anorganische Chemie, Ed. E. Riedel, C. Janiak, Vol. 7, **2007**, Berlin–New York: Walter de Gruyter.
- [57] C. E. Elwell, N. L. Gagnon, B. N. Neisen, D. Dhar, A. D. Spaeth, G. M. Yee, W. B. Tolman, *Chem. Rev.* **2017**, 2059–2107
- [58] A. de la Lande, H. Gérard, V. Moliner, G. Izzet, O. Reinaud, O. Parisel, *J. Biol. Inorg. Chem.* **2006**, *11*, 593–608.
- [59] A. E. Reed, R. B. Weinstock, F. Weinhold, *J. Chem. Phys.* **1985**, *83*, 735–746.
- [60] C. Meliá, S. Ferrer, J. Řezáč, O. Parisel, O. Reinaud, V. Moliner, A. de la Lande, *Chem. Eur. J.* **2013**, *19*, 17328–17337.
- [61] T. Abe, Y. Hori, Y. Shiota, T. Ohta, Y. Morimoto, H. Sugimoto, T. Ogura, K. Yoshizawa, S. Itoh, *Commun. Chem.* **2019**, *2*, Article number: 12. Further examples for nucleophilic superoxides include: a) W. D. Bailey, N. L. Gagnon, C. E. Elwell, A. C. Cramblitt, C. J. Bouchev, W. B. Tolman, *Inorg. Chem.* **2019**, *58*, 4706–4711. b) P. Pirovano, A. M. Magherusan, C. McGlynn, A. Ure, A. Lynes, A. R. McDonald, *Angew. Chem.* **2014**, *126*, 6056–6060; *Angew. Chem. Int. Ed.* **2014**, *53*, 5946–5950.
- [62] A. Hoffmann, M. Wern, T. Hoppe, M. Witte, R. Haase, P. Liebhäuser, J. Glatthaar, S. Herres-Pawlis, S. Schindler, *Eur. J. Inorg. Chem.* **2016**, 4744–4751.
- [63] L. Dahlenburg, H. Treffert, J. Dannhäuser, F. W. Heinemann, *Inorg. Chim. Acta* **2007**, *360*, 1474–1481
- [64] M. Findeisen, T. Brand, S. Berger, *Magn. Reson. Chem.* **2007**, 175–178.
- [65] G. R. Fulmer, A. J. M. Miller, N. H. Sherden, H. E. Gottlieb, A. Nudelman, B. M. Stoltz, J. E. Bercaw, K. I. Goldberg, *Organometallics* **2010**, 2176–2179.
- [66] B. Schulz, J. Bäckström, D. Budelmann, R. Maeser, M. Rübhausen, M. V. Klein, E. Schoeffel, A. Mihill, S. Yoon, *Rev. Sci. Instrum.* **2005**, *76*, 073107-1 – 073107-12.
- [67] B. Grimm-Lebsanft, C. Brett, F. Strassl, D. Rukser, M. Biednov, F. Biebl, M. Naumova, A. Hoffmann, L. Akinsinde, D. Brückner, S. Herres-Pawlis, M. Rübhausen, *Inorg. Chim. Acta.* **2018**, *481*, 176–180.
- [68] A. E. Sheshenev, M. S. Baird, A. K. Croft, I. G. Bolesov, *Tetrahedron* **2009**, *65*, 10036–10046; M. Oelgemöller, P. Cygon, J. Lex, A. G. Griesbeck, *Heterocycles* **2003**, *59*, 669–684.
- [69] DENZO-SMN, Nonius **1998**, <http://www.nonius.nl>.
- [70] G. M. Sheldrick, SADABS, *Program for Empirical Absorption Correction*, University of Göttingen, Germany.
- [71] a) G. M. Sheldrick, SHELXT, *Program for Crystal Structure Solution*, University of Göttingen, Germany **2014–2018**; b) G. M. Sheldrick, *Acta Cryst.* **2015**, *A71*, 3–8.
- [72] a) G. M. Sheldrick, SHELXL-20xx, *Program for Structure Refinement*, University of Göttingen, Germany **2014–2018**; b) G.M.Sheldrick, *Acta Cryst.* **2015**, *C71*, 3–8.
- [73] O. V. Dolomanov, L. J. Bourhis, R. J. Gildea, J. A. K. Howard, H. Puschmann, OLEX2: A complete structure solution, refinement and analysis program, *J. Appl. Cryst.* **2009**, *42*, 339–341.
- [74] a) P. v. d. Sluis, A. L. Spek, *Acta Cryst.* **1990**, *A46*, 194; b) A. L. Spek, *Acta Cryst.* **2015**, *C71*, 9.
- [75] a) A. L. Spek, *PLATON*, Utrecht University, The Netherlands; b) A. L. Spek, *J. Appl. Cryst.* **2003**, *36*, 7.

Entry for the Table of Contents

FULL PAPER

Metal cooperativity is suggested as the key to intramolecular ligand hydroxylation in a dinuclear copper complex.



F. Schön, F. Biebl, L. Greb, S. Leingang, B. Grimm-Lebsanft, M. Teubner, E. Kaifer, M. A. Rübhausen, H.-J. Himmel*

Page No. – Page No.

On the Metal Cooperativity
in a Dinuclear Copper-
Guanidine Complex for C–H
Bond Cleavage by Dioxygen